ASSESSMENT OF MECHANICAL PROPERTY GRADIENTS AFTER IMPACT-BASED SURFACE TREATMENTS USING NANO-COMPRESSION TESTING

D. Tumbajoy-Spinel[a, c], X. Maeder[b], J. Michler[b], S. Descartes[c],
J.M. Bergheau[d], V. Lacaille[e], C. Langlade[f], G. Kermouche[a*]
[a] Ecole des Mines de Saint-Etienne, LGF UMR5307 CNRS, Saint-Etienne, France, kermouche@emse.fr, [b] Empa, Swiss Federal Laboratories for Materials Science and Technology, Laboratory for Mechanics of Materials and Nanostructures, Feuerwerkerstr. 39, CH-3602 Thun, Switzerland [c] Université de Lyon, CNRS, INSA-Lyon, LaMCoS, UMR5259, F-69621 Villeurbanne, France, [d] Université de Lyon, ENISE, LTDS, UMR 5513 CNRS, F-42023 Saint-Etienne, France, [e] Winoa 528 Avenue de Savoie, BP3, 38570 Le Cheylas, France, [f] Université Technologique de Belfort-Montbéliard, IRTES-LERMPS EA 7274, 90010 Belfort, France.

Keywords: Shot-peening, Micro-percussion, Micro-pillar compression, Tribologically Transformed Surface (TTS), Mechanical surface treatment.

Introduction

Mechanical surface treatments are known to improve wear and fatigue resistance of metallic materials. In the case of conventional impact treatments (shot-peening [1]-[2], SMAT [3]), the surface is exposed to repeated mechanical loadings, producing near-surface severe plastic deformation (SPD). It leads to a local progressive refinement of the microstructure [2]-[3], commonly known as tribologically transformed structure (TTS) [4], and thus to a graded in-depth strengthening. Micro-percussion testing [5]-[6] appears to be an interesting model case scenario to emulate these conventional treatments and go further on micro-structural and mechanical characterization. For this technique, every impact is made at the same position by a rigid conical indenter, controlling the number, angle and velocity of each impact.
The aim of this paper is to describe and compare the mechanical and micro-structural gradients resulting of these two treatments. More precisely, three main goals are considered: (i) characterize the transformed surfaces; (ii) quantify the mechanical gradient in-depth by the means of local micro-mechanical testing (micro-pillar compression [7]-[8]); and (iii) compare both impact treatment effects evaluating the possibility to emulate industrial techniques with micro-percussion. This investigation is carried out using a pure α-iron.

Process and Methods: Shot-peening ant Micro-percussion tests in pure α-iron samples

Material: The mechanical surface treatments (shot-peening and micro-percussion) are done in a high-purity α-iron with less than 15 ppm of carbon. This material is produced by the cold crucible melting method. The resulting metallic bars are thermo-mechanically treated by forging and annealing at temperatures between 650 ºC and 800 ºC during 60 minutes. This technique leads to a homogeneous microstructure with average grain sizes of 250 µm and 1 mm for the shot-peening and the micro-percussion samples, respectively. Let us pay attention that no inclusions have been observed in this model material.
Shot-Peening: this mechanical surface treatment had been carried out in collaboration with Winoa group (France) using one of their main industrial procedures: nano-peening® [9]-[11]. The principle of this technique is to project repeatedly hard steel balls (0.1 mm to 2 mm diameter) towards the sample surface (Figure 1-a) [1]-[2]. The impact tilt could vary from 10º to 45º and the projection speeds could take high values in the order of 50 m/s to 100 m/s. In this case, a surface coverage of 5000 % had been used. The severe plastic deformation (SPD) induced by this treatment leads to a micro-structural transformation (grain refinement) and to a local strengthening in the near-surface.
Micro-percussion tests: the principle is to carry out several impacts at the same position using a rigid conical punch made of carbide tungsten (Figure 1-b) [5]-[6]. The indenter tip has a spherical shape with a radius of 0.5 mm and an angle of 60º. The SPD leads to a remaining imprint of mm size. The

impact set-up allows controlling impacts number and speed [12]. On the contrary, the impact angle is introduced directly on the sample geometry with a tilted surface. In preliminary experiments [13], several tests had been done taking into account different impact conditions: (i) angles varying from 0º to 30º, (ii) number of impacts between 10 and 10000 and (iii) velocities between 80 mm/s and 200 mm/s [12]. A parameter sensitivity analysis had pointed out that the remaining print, as well as the transformed micro-structure, grows progressively with the number of impacts (Figure 1-b). In this work, the print obtained at 15º, 10000 impacts and a velocity of 150 mm/s had been chosen to analyse the micro-structural transformation and the local strengthening. Surface characterizations and micro-mechanical testing results are compared with those measured in samples treated by the means of shot-peening.

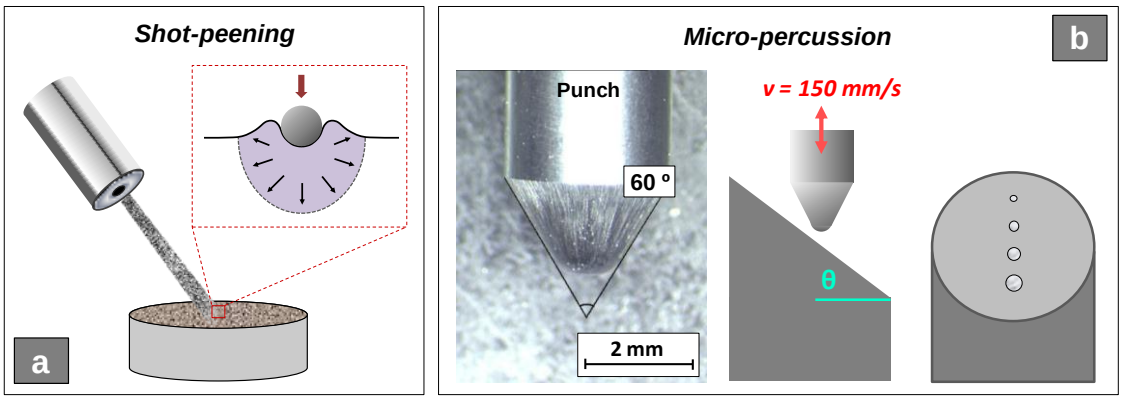

Figure 1. Schematic representations of (a) the shot-peening treatment and (b) the micro-percussion testing.

Micro-structural characterization

The characterizations of the resulting surfaces were done using scanning electron microscopy (SEM) and electron back-scattered diffraction (EBSD) mapping. Both techniques were carried out on samples cross-section to observe the near-surface micro-structural evolution. For both techniques, samples were cutted-off with a metallic wire saw and then mechanically polished up to the middle plane. The surfaces were polished with different abrasive papers (P240 to P1200), two diamond suspensions (3 µm and 1 µm) and finished with colloidal silica. The SEM images were done in a Zeiss Supra 55 VP at 20 kV using a back-scattered detector (BSE). The EBSD maps were carried out in a Tescan Lyra3/XMU (FEG/FIB) using an indexation step of 120 nm and 300 nm for the shot-peening and the micro-percussion samples, respectively.

Cross-section global view: the SEM images (Figure 2) show a global characterization of the cross section of the shot-peening and the micro-percussion surfaces. In the case of shot-peening (Figure 2-a), three main regions are observed. The first zone corresponds to the TTS, formed by refined sub-micrometric grains (>1 µm) in the near surface [4]. The thickness of this region varies approximately from 30 µm to 80 µm. This layer is followed below by a transition zone, where no new refined grains are formed in spite of the induced SPD [14]. Indeed, the TTS layer and the transition zone make up the mechanically affected zone (MAZ) [15], formed by the impact-based treatment. The virgin bulk material without transformation is observed beyond this MAZ.

Concerning the micro-percussion sample, the MAZ seems to be at least twice the plastically deformed region obtained by shot-peening. Indeed, the width of the TTS layer is in the order of 100 µm. This region is formed by refined sub-micrometric grains as well as the shot-peening sample. Beyond the TTS layer, two more regions are stood out in the MAZ: (i) the transition zone and (ii) the "low angle boundaries" (LAB's) region [16]. On the one hand, the transition zone corresponds to the joint between a poly-crystal region (TTS zone) and a single-crystal local microstructure (considering the large grain sizes of the bulk: ~1 mm). On the other hand, the LAB's layer

corresponds to a single crystal region where slight crystal misorientations emerge into the material as a consequence of the impact-based SPD [16]-[17]. The difference between these two layers is nearly unrecognizable in the shot-peening sample because of the smaller width of the MAZ.

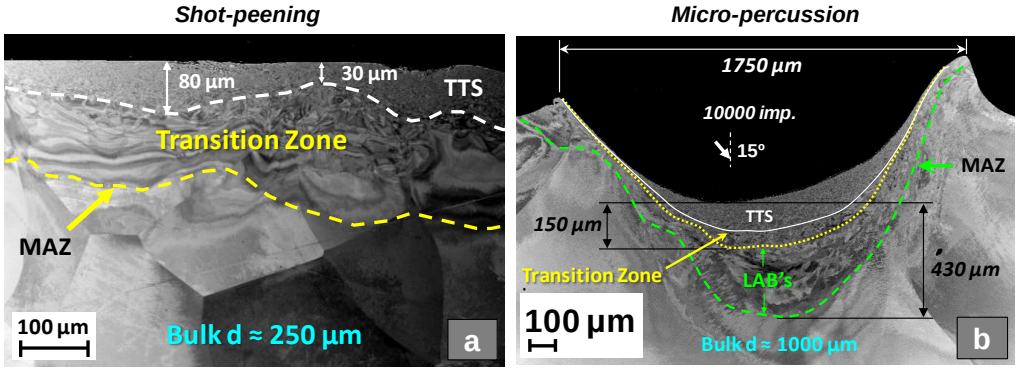

Figure 2. Global view of the cross-section (SEM images) of the resulting (a) shot-peening surface and (b) the micro-percussion imprint.

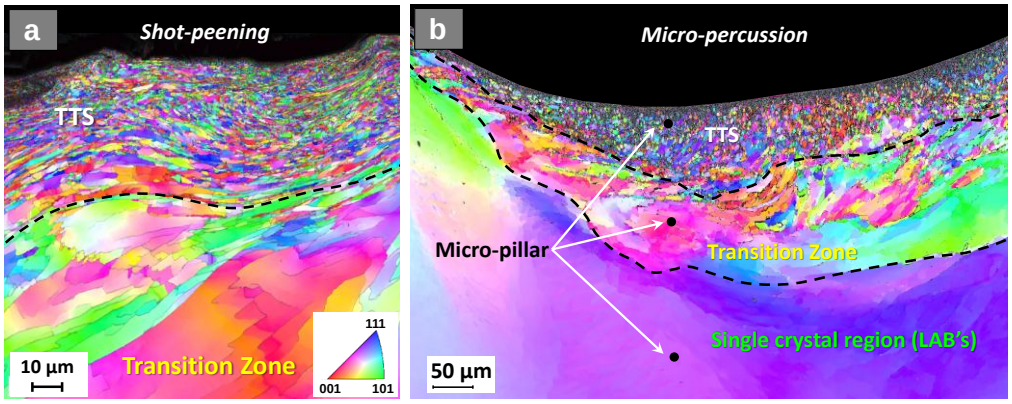

Figure 3. EBSD mapping on the cross-section of the transformed surfaces by the means of (a) Shot-peening and (b) Micro-percussion testing.

Local micro-structural characterization: the EBSD mapping permits as well to describe the micro-structural gradient in-depth produced by the SPD. The cross-section regions previously identified are locally disclosed in the EBSD maps of Figure 3. From both techniques, the TTS layers are qualitatively similar in morphology, texture and grain sizes. More precisely, for the shot-peening sample, the grain sizes increases from 0.75 µm to 6 µm at the border of the TTS region, i.e. at 60 µm from the near-surface. By contrast, the grain size gradient for the micro-percussion sample varies from 1 µm in the near-surface up to 4 µm at 100 µm in-depth. These statistics reveal that the grain refinement is in the same order for both TTS regions in spite of the micro-percussion impacts can produce wider layers. Concerning the transition zone, significant crystal misorientations are pointed out although grain boundaries are not well-defined anymore [14]. Furthermore, the single crystal zone presents low angle boundaries (LAB's) as described before. As schematically presented in Figure 3-b, the mechanical gradient associated to the micro-structural transformation is measured throughout all these zones by micro-pillar compression testing.

Mechanical gradient measured by micro-pillar compression testing

Fabrication: micro-pillar compression testing leads to measure the true stress-strain behaviour at very local positions and accurately assess the mechanical gradient in-depth [18]. As shown in Figure 4-a, the pillars were carried out on the cross-section of the samples. Micro-pillars were milled by the means of gallium source focused ion beam (FIB) [7],[8],[18]. Two microscopes were used for that purpose: (i) the Zeiss NVision40 for the shot-peening sample and (ii) the FEI Helios NanoLAB 600i Dual Beam for the micro-percussion sample. The milling rates of the gallium beam were used between ca. 0.28 μm^2/nA/s and ca. 0.12 μm^2/nA/s at 30 kV, depending on the crystal orientations and the micro-structural features. Indeed, the poly-crystal layers are heterogeneously milled because of the various crystal orientations and different mechanical properties (Figure 4-b). In contrast, the milling process in single-crystal regions is quite homogeneous (Figure 4-f). The general machining process includes 3 rough milling phases with currents decreasing from 27 nA to 800 pA. The final polishing step takes currents from 700 pA to 280 pA. This strategy permits to obtain clean and homogeneous pillar surfaces.

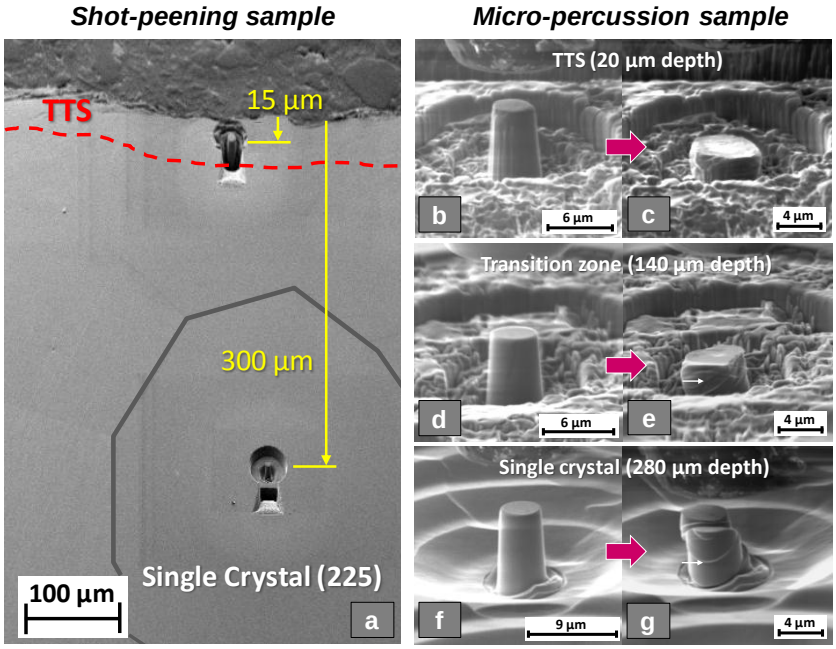

Figure 4. (a) 2 Micro-pillars on the cross section of the sample treated by shot-peening. 3 Tests on the micro-percussion sample throughout different layers: (b, c) TTS, (d, e) transition and (f, g) single-crystal.

For the shot-peening sample, two pillars were produced in the TTS and the bulk material regions (Figure 4-a). The TTS pillar is located at 15 µm depth, and is in a poly-crystalline region of ca. 800 nm average grain size. The bulk pillar is produced at 300 µm depth, i.e. on a single crystal region with an orientation of ⟨225⟩ with respect to the load direction. The geometrical aspects ratios are of 2.6 for the TTS pillar (9.3 µm diameter and 24 µm height) and 1.9 for the bulk material pillar (5.4 µm diameter and 10.4 µm height). These pillars have a tapered angle of 2.5º and 4.5º for the TTS and bulk regions, respectively. Concerning the micro-percussion sample, three pillars have been done (Figure 4-b,d,f) along the three regions previously identified in Figure 3-b: the TTS (at 20 µm depth), the transition zone (at 140 µm depth) and the single-crystal region (at 280 µm depth). These pillars were done considering a geometrical ratio of 2 (ca. 4 µm diameter and ca. 8 µm height). Moreover, pillars have a conical shape with an average tapered angle of 4.3º. Note that the single-crystal pillar was done on the crystal orientation $\langle 84\bar{3} \rangle$ with regards to the loading direction.
Compression testing and results: all *in situ* compression tests (within a SEM) were carried out using an Alemnis nano-indentation set-up [19]. Micro-compressions had been done with a load-unload

rate of 0.03 µm/s using flat punches of 15 µm and 10 µm diameter according to the pillar dimensions. As shown in Figure 4, the pillar deformation is completely different according to the micro-structural nature. For the TTS pillar (Figure 4-c), deformation is entirely homogeneous as expected. On the opposite, the bulk pillar (Figure 4-g) deforms in well-defined glide planes (white arrows) following the activated preferential slip systems [20]. Concerning the transition pillar (Figure 4-e), it tends to deform in a middle way between the last two extreme cases. Pillars deformation is likely uniform although some slip planes are clearly visible.
The true stress-strain curves are presented in Figure 5-a. These curves have been plotted accounting of punch and frame [8],[19]. Dashed-lines correspond to the shot-peening sample, while continuous lines correspond to the micro-percussion sample. The mechanical gradient evolves throughout the different micro-structural regions: the TTS (red lines), the transition zone (magenta line) and the single-crystal material (blue lines).

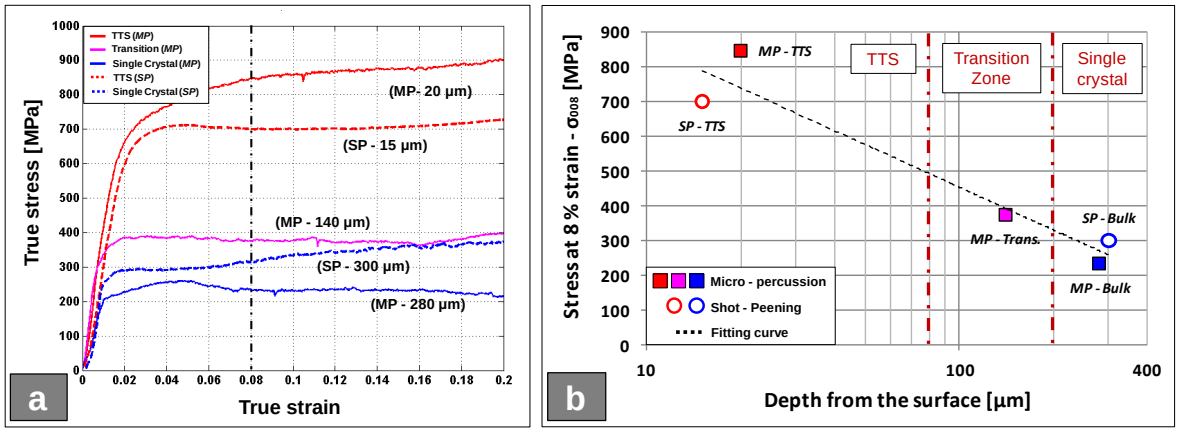

Figure 5. (a) True stress-strain curves from the micro-pillar compression tests. (b) Stress at 8 % of strain in function of the depth from the near-surface.

Similarly to macroscopic compression test, micro-compression cannot allow a precise measurement of the elastic modulus and the yield strength of metallic materials. For this reason, it has been chosen to use the yield stress at 8 % of strain ($\sigma_{0.08}$) to compare the mechanical gradients in both samples [21]. The $\sigma_{0.08}$ stresses are plotted versus the distance to the near-surface throughout the different layers (semi-log plot in Figure 5-b). The experimental data follows a power law ($\sigma_{0.08} \approx -180\ln(z) + 1270$, with z the distance to the surface). For both kinds of surfaces, the TTS pillars have an average yield stress of 770 MPa. The pillar in the transition zone exhibits a yield strength of ca. 375 MPa whereas pillars in the single-crystal region have a mean strength of ca. 270 MPa. The discrepancy on the TTS local properties should be related to a microstructural effect, despite mean grain sizes are nearly similar. In the case of single crystal pillars, the discrepancy could be associated to the different crystal orientations with respect to the load sense.

Conclusions

In this work, an innovating approach based on the combination of mechanical and micro-structural characterisation techniques were used to contrast two different impact treatments. This analysis pointed out that the micro-percussion test could be an interesting method to emulate the mechanical and micro-structural gradients induced by the means of conventional industrial techniques (as shot-peening) [1]-[3]. Grain refinement from both techniques produced TTS layers with similar average grain sizes, morphologies and textures. However, it had been shown that the micro-percussion process could lead to larger mechanically affected zones (MAZ) and slightly

thicker TTS layers. Some previous works had revealed that this phenomenon could be probably related to the impact conditions : impact angles, number of impacts, impact energy [13]. Indeed, the tilted impacts could favour some micro-structural transformation mechanisms (dislocation mobility [17], micro-shear bands [22], ...) in materials with high stacking fault energy (as pure α-iron). In reference to the mechanical characterization, the mechanical gradients ($\sigma_{0.08}$) decrease progressively from the near-surface to the bulk material. Note that both mechanical gradients are nearly comparable and are in agreement with the mechanical gradient identified by nano-indentation testing in a previous work [11]. Comparing the Berkovich hardness (H) to its representative strength ($\sigma_{0.08}$), the relations are nearly close to the Tabor's expression: $H/\sigma_{0.08} \approx 3$ [21]. Moreover, the mechanical discrepancies observed for the TTS pillars and the single-crystal pillars might be related to its micro-structural nature. To conclude, future works would aim a quantitative match between the mechanical and microstructural gradients in order to reveal the influence of different strengthening mechanisms (the Hall-Petch effect [11], the work hardening [23]-[24], ...). This analysis might elucidate why the mechanical gradients are quite similar in-depth, even though the micro-percussion technique could produce thicker affected zones.

Acknowledgment
This work is supported by the LABEX MANUTECH-SISE (ANR-10-LABX-0075) of Université de Lyon, within the program "Investissements d'Avenir" (ANR-11-IDEX-0007) operated by the French National Research Agency (ANR). The authors would like to thank Dr. Halim Al-Baida (UTBM, France) and Dr. Constance Morel (Winoa, France) for their expertise and help on the micro-percussion and shot-peening sample preparation, respectively.

References

[1] Nordin E and Alfredsson B 2016 *Journal of Materials Processing Technology* **235** 143–148
[2] Marteau J and Bouvier S 2016 *Surface & Coatings Technology* **296** 136–148
[3] Lu K and Lu J 2004 *Materials Science and Engineering A* **375**–377 38–45
[4] Descartes S, Busquet M and Berthier Y 2011 *Wear* **271** 1833-1841
[5] Al-Baida H, Langlade C, Kermouche G and Ambriz R-R 2015 *J. Mater. Res.* **30** 2222-2230
[6] Kermouche G, Pacquaut G, Langlade C and Bergheau J-M 2011 *C. R. Mecanique* **339** 552–562
[7] Monnet G and Pouchon M-A 2013 *Materials Letters* **98** 128–130
[8] Greer J-R, Oliver W-C, and Nix W-D 2005 *Acta Materialia* **53** 1821–1830
[9] Lacaille V, Kermouche G, Tumbajoy-Spinel D, Feulvarch E, Morel C and Bergheau J-M 2014 *IOP Conf. Series: Materials Science and Engineering* **63** 012124
[10] Tumbajoy-Spinel D, Kermouche G, Descartes S, Bergheau J.-M, Lacaille V, Guillonneau G and Michler J 2015 *Matériaux & Techniques* **103 303**
[11] Tumbajoy-Spinel D, Descartes D, Bergheau J-M, Lacaille V, Guillonneau G, Michler J and Kermouche G 2016 *Materials Science and Engineering A* **667** 189–198
[12] Al-Baida H, Langlade C, Kermouche G and Ambriz R-R 2014 *Matériaux & Techniques* **102 604**
[13] Tumbajoy-Spinel D, Descartes S, Bergheau J-M, Al-Baida H, Langlade C, Kermouche G 2017 *IOP Conf. Series: Materials Science and Engineering* **In-Press**
[14] Tao N-R, Wang Z-B, Tong W-P, Sui M-L, Lu J and Lu K 2002 *Acta Materialia* **50** 4603–4616
[15] Juran P, Liotier P-J, Maurice C, Valiorgue F and Kermouche G 2015 *C. R.Mecanique* **343** 344–353
[16] Sakai T, Belyakov A, Kaibyshev R, Miura H and Jonas J 2014 *Progress in Materials Science* **60** 130–207
[17] Kubin L-P and Mortensen A 2003 *Scripta Materialia* **48** 119 – 125
[18] Sun Z, Retraint D, Guelorget B and Waltz L 2015 *Matériaux & Techniques* **103 304**
[19] Rabe R, Breguet J-M, Schwaller P, Stauss S, Haug F-J, Patscheider J, and Michler J 2004 *Thin Solid Films* **469 - 470** 206 – 213
[20] Soras-Rogne B-R and Thaulow C 2015 *Materials Science & Engineering A* **621** 133–142
[21] Dao M, Chollacoop N, Van Vliet K-J, Venkatesh T-A, and Suresh S 2001 *Acta Materialia* **49** 3899 – 3918
[22] Segal V-M 2005 *Materials Science and Engineering A* **406** 205–216
[23] Frutos E, Multigner M and González-Carrasco J-L 2010 *Acta Materialia* **58** 4191–4198
[24] Zou Y, Maiti S, Steurer W and Spolenak R 2014 *Acta Materialia* **65** 85–97